ЖЭТФ, 2004, том 125, вып. 5, стр. 1122–1127

ON THE HIGH-PRESSURE BEHAVIOR OF THE BOND-BENDING MODE OF AlN

E. V. Yakovenko *

Institute for High-Pressure Physics, Russian Academy of Sciences
142190, Troitsk, Moscow Region, Russia

M. Gauthier **, ***A. Polian*** ***

Physique des Milieux Condensés, Université P&M Curie
F 75252, Paris Cedex 05, France

Submitted 8 July 2003

Lattice vibrations of the wurtzite-type AlN have been studied by Raman spectroscopy under high pressure up to the phase transition to the rock salt structure at 20 GPa. Five fundamental bands E_2^2, $A_1(TO)$, $E_1(TO)$, $A_1(LO)$, and $E_1(LO)$ have a strong, positive pressure shift, whereas the shift of the low-frequency E_2^1 band is weakly positive. We have found that the bond-bending E_2^1 mode has a positive mode Grüneisen parameter $\gamma_i = 0.04$, which is qualitatively consistent with the recently reported value $\gamma_i = 0.12$ [21]. Thus, we confirm that AlN remains stable with respect to the bond-bending mode, while in most tetrahedral semiconductors bond-bending modes soften on compression. Experimental results are compared with the first-principle calculations.

PACS: 63.20.Dj, 64.70.Kb

The pressure-induced phonon softening is a significant characteristic property of tetrahedral semiconductors, reported in many experimental [1–10] and theoretical [11–18] works. Negative frequency shift of the low-energy modes of tetrahedral semiconductors on compression manifests itself in their well-known negative thermal expansions at low temperatures. These «soft» modes are shearing modes, involving bond bending in the first order of the strain [15, 18]. Phonon frequency drop, more pronounced for high-Z materials, reaches about 30 % at the threshold of the pressure-induced phase transitions, when covalent tetrahedral structures lose their stability and transform into more densely packed arrangements. Experimentally, it has been found that the stability of tetrahedral structures with respect to the bond-bending modes correlates with their absolute stability under pressure such that the frequency drop is faster for less stable compounds. Weinstein [4, 6] has found that for six diamond and zinc-blende structure semiconductors ZnTe, Ge, Si, ZnSe, ZnS, and GaP, there is a remarkable linearity between the mode Grüneisen parameter

$$\gamma_i = -\frac{d\ln\nu_i}{d\ln V}$$

(where ν_i is the frequency of the mode i and V is the volume) for the purely bond-bending $TA(X)$ mode and the transition pressure P_{tr} for these materials.

Previously, the only known experimental examples of bond-bending modes with a positive pressure shift were the bond-bending $TA(X)$ mode of diamond [19][1)] and the E_2^1 mode of wurtzite-type BeO [20]. This behavior might be regarded as characteristic feature of the low-Z second-row semiconductors; however, recent Raman measurements found a similar behavior for the E_2^1 mode of the wurtzite-type AlN (w-AlN) at pressures to up 6 GPa [21]. Previous high-pressure Raman studies of w-AlN [22, 23] failed to measure the pressure

*E-mail: katia@ns.hppi.troitsk.ru
**E-mail: Michel.Gauthier@pmc.jussieu.fr
***E-mail: Alain.Polian@pmc.jussieu.fr

[1)] We note that the experimental error bar for $\gamma_{TA}(X)$ for diamond obtained in this work is twice the value of $\gamma_{TA}(X)$ itself. However, the positive sign of $\gamma_{TA}(X)$ is indirectly corroborated by the positive thermal expansion coefficient of diamond at low temperatures.

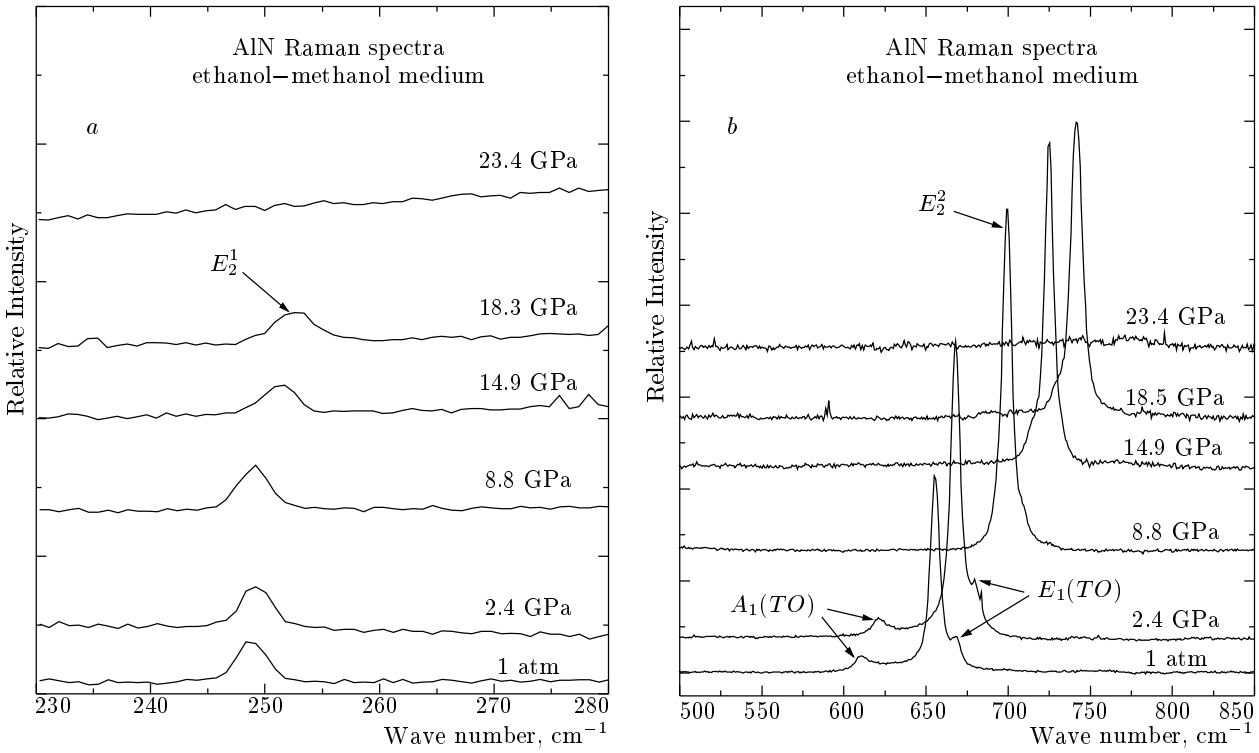

Fig. 1. Raman spectra of AlN as a function of pressure in the low-energy region (a) and in the high-energy region (b). The spectral resolution is 0.5 cm^{-1}. Ethanol–metanol mixture was used as a pressure transmitting medium

shift of the E_2^1 mode, most probably due to the lack of high-quality crystals. We believe that this problem deserves special attention, because the bond-bending elasticity is one of the most prominent manifestations of directional covalent bonding, and its pressure behavior should be studied in depth. From a fundamental standpoint, AlN represents an interesting and complicated case of covalent versus ionic bonding [24]: although its valence charge distribution is highly ionic [25], AlN adopts the tetrahedrally coordinated wurtzite structure and therefore belongs to covalent materials [26]. To ensure that the pressure coefficient of the E_2^1 mode of AlN is indeed positive, we have taken a complementary high-pressure Raman study of AlN up to its stability limit at about 20 GPa. The pressure dependence of the low-frequency bond-bending E_2^1 mode was traced up to the threshold of the pressure-induced phase transition for the first time.

The AlN samples were 20 μm-thick crystals grown on the sapphire substrate by vapor phase epitaxy. Pressure was produced using the diamond-anvil pressure cell. Compressed helium and methanol–ethanol mixture were used as a pressure-transmitting medium in the first and in the second experimental run, respectively. Pressure was measured *in situ* by the ruby luminescence technique. The Raman spectra were measured using the THR-1000 triple spectrometer equipped with an OSMA detector (the first run), and the Dilor XY double spectrometer equipped with the CCD detector (the second run). An Ar^+ laser ($\lambda = 514.5$ nm) was used as a source of excitation. All spectra were recorded in the backscattering geometry at ambient temperature.

For the hexagonal wurtzite structure with the space group $P6_3mc$ ($Z = 2$), a factor-group analysis predicts the six sets of optical modes at $k = 0$ [27],

$$\Gamma_{op} = A_1 + 2B_1 + E_1 + 2E_2,$$

where A_1, E_1, and E_2 are Raman active modes, and B_1 modes are silent. A_1 and E_1 are also infrared active, and split into the longitudinal and transverse components (LO and TO). The lowest-frequency mode E_2^1 is a bond-bending mode.

The Raman spectrum of w-AlN has been measured previously under ambient conditions and analyzed in some detail, including the effects of polarization and anisotropy [28–30]. Our ambient pressure Raman frequencies are 249 cm^{-1}, 610 cm^{-1}, 657 cm^{-1}, 669 cm^{-1},

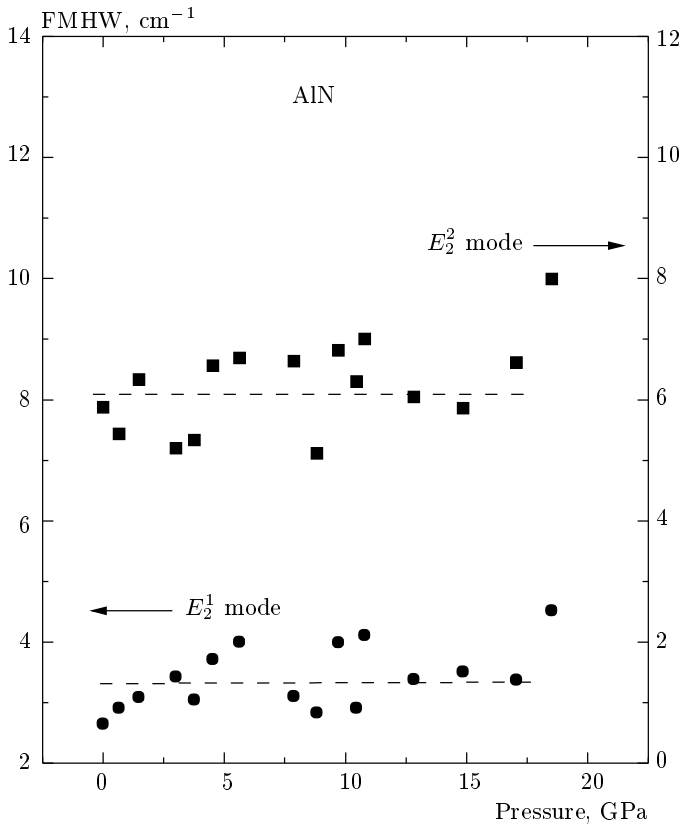

Fig. 2. Raman band width (FMHW) for the E_2^1 and E_2^2 modes of AlN as a function of pressure. Ethanol–metanol mixture was used as a pressure transmitting medium. The dashed horizontal lines are drawn to guide the eye

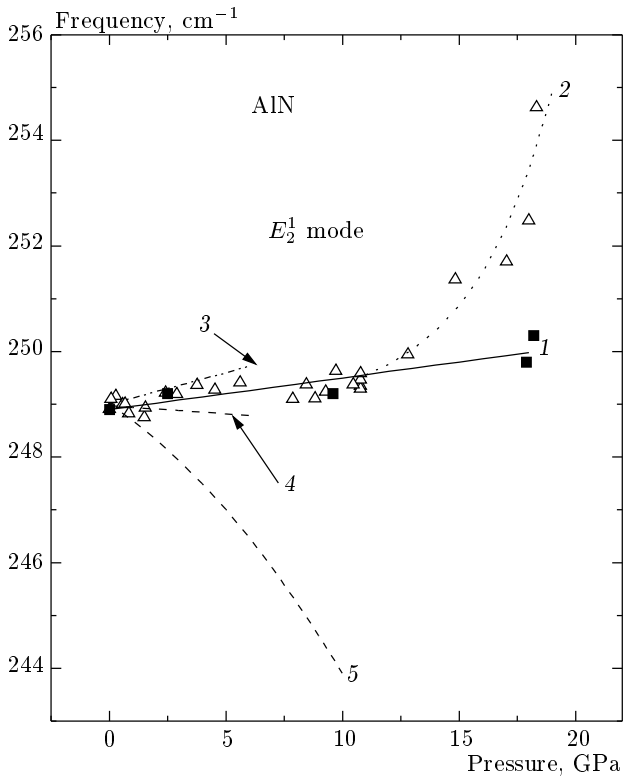

Fig. 3. Comparison between the measured and calculated pressure dependence of the Raman frequency for the E_2^1 mode of AlN. The squares are the first run data, obtained with compressed helium as a pressure transmitting medium. The triangles are the second run data, obtained with ethanol–methanol mixture as a pressure transmitting medium. Solid line *1* is a linear fit of the first run data. Dotted line *2* is a guide for the eye. Line *3* is the experimental dependence obtained in Ref. [21]. Lines *4* and *5* are the calculated dependences obtained in Ref. [21] and Ref. [33], respectively. All data are shifted along the vertical axis in order that the ambient pressure frequencies coincide with the value 249 cm^{-1} obtained in our experiment

890 cm^{-1}, and 910 cm^{-1} for the respective modes E_2^1, $A_1(TO)$, E_2^2, $E_1(TO)$, $A_1(LO)$, and $E_1(LO)$. These values agree with very reliable data [28–30] within 1 %. On increase in pressure, all Raman bands shift continuously to higher phonon energy with neither broadening nor intensity loss to about 18 GPa. Above 18 GPa, the bands weaken and disappear at about 21 GPa in both experimental runs due to the phase transition to the rock salt structure [31, 32]. Representative Raman spectra of AlN in the low- and high-energy region as a function of pressure are shown in Fig. 1. Pressure dependences of the E_2^1 and E_2^2 band widths are shown in Fig. 2.

Figure 3 compares measured and calculated pressure dependences of the Raman frequency for the E_2^1 mode of AlN. In our experiment, the pressure dependence of the E_2^1 frequency is weak but apparently positive and linear up to 13 GPa in both runs. Above 13 GPa, the first run data fall well on the low-pressure dependence, while the second run data indicate a sudden rise of the E_2^1 frequency. This is possibly associated with solidification of the ethanol–methanol medium, resulting in a nonhydrostatic sample stress. Therefore, above 13 GPa, the first run data obtained in hydrostatic conditions with compressed helium as a pressure transmitting medium are the most reliable ones. We note that solidification of the ethanol–methanol medium did not result in any detectable anomaly of the pressure dependence of the high-frequency bond-stretching modes (see Fig. 4). We believe that the nonhydrostatic stresses result in a much weaker response of these modes in comparison to their strong dependence on the high hydrostatic pressure.

Table 1. Measured and calculated linear pressure coefficients ν_i' [$\text{cm}^{-1} \cdot \text{GPa}^{-1}$] obtained for the AlN Raman frequencies

	E_2^1	$A_1(TO)$	E_2^2	$E_1(TO)$	$A_1(LO)$	$E_1(LO)$
Experiment						
Present 1	0.05(1)	3.8(2)	4.9(2)	4.5(1)	–	–
Present 2	0.05(1)	4.3(2)	4.65(3)	4.55(6)	4.0(1)	3.6(7)
[21]	0.12(5)	4.4(1)	4.99(3)	4.55(3)	–	4.6(1)
Calculations						
[33]	−0.29	4.29	4.79	4.36	–	–
[21]	−0.03	3.0	4.2	3.8	3.5	4.0

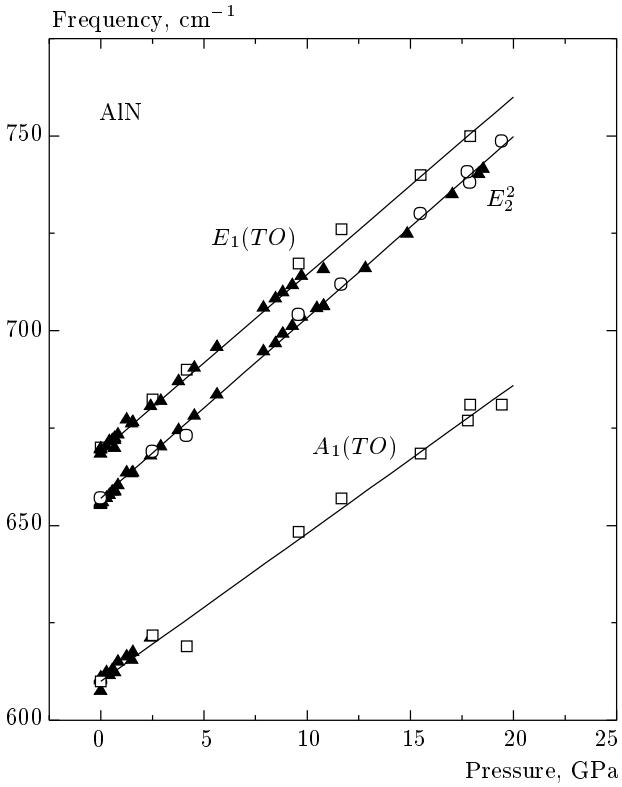

Fig. 4. The measured pressure dependence of the Raman frequency for the E_2^2 and TO modes of AlN. The squares and circles are the first run data, obtained with compressed helium as a pressure transmitting medium. The triangles are the second run data, obtained with ethanol–methanol mixture as a pressure transmitting medium. The solid lines are linear fits of the first run data

The mode pressure coefficients ν_i' calculated using the linear least-square fit

$$\nu_i = \nu_{i0} + \nu_i' P,$$

where ν_i is the frequency of the mode i at the pressure P, are listed in Table 1. The E_2^1 frequency in the second run was fitted only to 12 GPa. Our mode pressure coefficients ν_i' are consistent with the results reported in Ref. [21], although with somewhat lower pressure slope for the E_2^1 frequency (see Table 1).

Ab initio calculations [21, 33] give a weak negative pressure shift for the E_2^1 mode of AlN. Nevertheless, the pressure coefficient of the E_2^1 mode is nearly zero, and the differences between experimental and calculated pressure shifts are quite small on the absolute scale. The agreement between measured and calculated coefficients of the E_2^2, TO, and LO modes is very satisfactory (see Table 1).

As we mentioned earlier, the bond-bending phonon modes of most tetrahedral semiconductors soften under compression and thus have negative Grüneisen parameters γ_i. Table 2 compiles experimental mode Grüneisen parameters obtained on the basis of the first- and the second-order Raman measurements and inelastic neutron scattering for the bond-bending modes in a series of tetrahedral compounds. The calculated Grüneisen parameters for diamond and BP are also displayed. A negative value of γ_i is observed in most cases except for diamond, BeO, and AlN. For BP, calculations [36] predict an exotic combination of negative γ_i for the bond-bending $TA(X)$ mode and positive γ_i for the bond-bending $TA(L)$ mode. The E_2 mode of SiC-6H has zero pressure slope and hence zero γ_i, but the quadratic pressure coefficient of the mode frequency is negative [7]. We thus see that AlN is one of the most stable materials with respect to the bond-bending mode on compression.

Despite this, w-AlN undergoes a first-order phase transition to the rock-salt structure at a rather low pressure of 20 GPa. At the same time, SiC-6H and

Table 2. Mode-Grüneisen parameters γ_i for the bond-bending modes in a series of $A^N B^{8-N}$ compounds (W — wurtzite structure, ZB — zinc blende structure, D — diamond structure, L — hexagonal diamond structure)

Material	Structure	Mode	γ_i	Reference
Experiment				
CdS	W	E_2^1	-2.7	[6]
InP	ZB	$TA(L)$	-2.0	[6]
ZnO	W	E_2^1	-1.8	[6]
GaAs	ZB	$TA(L)$	-1.7	[6]
ZnSe	ZB	$TA(L)$	-1.5	[6]
ZnS	ZB	$TA(L)$	-1.5	[6]
Ge	D	$TA(L)$	-1.52	[10]
Si	D	$TA(L)$	-1.3	[3]
ZnTe	ZB	$TA(L)$	-1.0	[6]
GaP	ZB	$TA(L)$	-0.81	[2]
GaN	W	E_2^1	-0.426	[8]
SiC-6H	Hex.	E_2	0.0	[7]
BeO	W	E_2^1	0.04	[20]
AlN	W	E_2^1	0.04	This study
			0.10	[21]
C	D	$TA(X)$	0.4	[19]
Calculations				
C	D	$TA(X)$	0.3	[34]
C	D	$TA(L)$	0.17	[34]
C	L	E_{2u}	0.16	[35]
BP	ZB	$TA(X)$	-0.64	[36]
			-0.27	[37]
BP	ZB	$TA(L)$	0.121	[36]

w-BeO, which have nearly the same values of γ_i for the bond-bending E_2 modes as AlN, preserve the tetrahedral structures up to the pressures as high as 100 GPa [38] and 140 GPa [39], respectively. This obviously indicates that the applicability of Weinstein's empirical correlation rule [4, 6] is limited.

The pressure behavior of the bond-bending modes of tetrahedral semiconductors can be elucidated in terms of the pressure-sensitive balance between stabilizing and destabilizing contributions to the restoring force constants [15]. This balance, in turn, can be traced back to the atomic configuration of the constituent atoms, as this has been done in the analysis of the thermodynamical stability of the diamond phase of carbon [40]. However, this issue is beyond the scope of the present report and will be discussed in a following paper.

The authors wish to thank A. Dobrynin for growing the AlN crystals. E. V. Yakovenko is grateful to A. F. Goncharov for his assistance in Raman measurements.

REFERENCES

1. R. T. Payne, Phys. Rev. Lett. **13**, 53 (1964).

2. B. A. Weinstein and G. J. Piermarini, Phys. Lett. A **48**, 14 (1974).

3. B. A. Weinstein and G. J. Piermarini, Phys. Rev. B **12**, 1172 (1975).

4. B. A. Weinstein, Sol. St. Comm. **24**, 595 (1977).

5. D. Olego and M. Cardona, Phys. Rev. B **25**, 1151 (1982).

6. B. A. Weinstein and R. Zallen, in *Light Scattering in Solids IV*, ed. by M. Cardona and G. Guntherodt, Springer & Heidelberg (1984), p. 463.

7. E. V. Yakovenko, A. F. Goncharov, and S. M. Stishov, High Press. Res. **7**, 433 (1991).

8. P. Perlin, C. Jauberthie-Carillon, J. P. Itié et al., Phys. Rev. B **45**, 83 (1992).

9. H. Olijnyk, High Press. Res. **10**, 461 (1992).

10. S. Klotz, J. M. Besson, M. Braden et al., Phys. Rev. Lett. **79**, 1313 (1997).

11. G. Dolling and R. A. Cowley, Proc. Phys. Soc. **88**, 463 (1966).

12. R. M. Martin, Phys. Rev. **186**, 871 (1969).

13. H. Jex, Phys. Stat. Sol. (b) **45**, 343 (1971).

14. H. Wendel and R. M. Martin, Phys. Rev. B **19**, 5251 (1979).

15. M. T. Yin and M. L. Cohen, Phys. Rev. B **26**, 3259 (1982); **26**, 5668 (1982).

16. K. J. Chang and M. L. Cohen, Phys. Rev. B **31**, 7819 (1985); **34**, 8581 (1986).

17. O. H. Nielsen, Phys. Rev. B **34**, 5808 (1986).

18. D. J. Chadi and R. M. Martin, Sol. St. Comm. **19**, 643 (1976).

19. B. J. Parsons, Proc. Roy Soc. London A **352**, 397 (1977).

20. A. P. Jephcoat, R. J. Hemley, H. K. Mao et al., Phys. Rev. B **37**, 4727 (1988).

21. A. R. Goñi, H. Siegle, K. Syassen et al., Phys. Rev. B **64**, 035205 (2001).

22. J. A. Sanjurjo, E. Lopez-Cruz, P. Vogl et al., Phys. Rev. B **28**, 4579 (1983).

23. P. Perlin, A. Polian, and T. Suski, Phys. Rev. B **47**, 2874 (1993).

24. K. Karch and F. Bechstedt, Phys. Rev. B **56**, 7404 (1977).

25. E. Gabe, Y. LePage, and S. L. Mair, Phys. Rev. B **24**, 5634 (1981).

26. W. Harrison, *Electronic Structure and Properties of Solids*, Freeman, San Francisco (1980).

27. W. G. Fateley, F. R. Dollish, N. T. McDevitt et al., in *Infrared and Raman Selection Rules for Molecular and Lattice Vibrations: The Correlation Method*, Wiley-Interscience, New York (1972).

28. L. E. McNeil, M. Grimsditch, and R. H. French, J. Amer. Ceram. Soc. **76**, 1132 (1993).

29. L. Filippidis, H. Siegle, A. Hoffman et al., Phys. Stat. Sol. (b) **198**, 621 (1996).

30. V. Yu. Davydov, Yu. E. Kitaev, I. N. Goncharuk et al., Phys. Rev. B **58**, 12899 (1998).

31. M. Ueno, A. Onodera, O. Shimomura et al., Phys. Rev. B **45**, 10123 (1992).

32. Q. Xia, H. Xia, and A. L. Ruoff, J. Appl. Phys. **73**, 8198 (1993).

33. I. Gorczyca, N. E. Christensen et al., Phys. Rev. B **51**, 11936 (1995).

34. J. Xie, S. P. Chen, J. S. Tse et al., Phys. Rev. B **60**, 9444 (1999).

35. B. R. Wu and Ji-an Xu, Phys. Rev. B **60**, 2964 (1999).

36. D. N. Talvar, G. Thaler, S. Zaranek et al., Phys. Rev. B **55**, 11293 (1977).

37. H. W. Leite Alves, and K. Kunc, J. Phys. Condens. Matter **4**, 6603 (1992).

38. M. Yoshida, A. Onodera, M. Ueno et al., Phys. Rev. B **48**, 10587 (1993).

39. Y. Mori, T. Ikai, K. Takarabe, in *Abstracts of High Pressure Conference of Japan* (2002), *Special Issue of the Review of High Pressure Science and Technology* **12**, 2D05 (2002).

40. M. T. Yin and M. L. Cohen, Phys. Rev. Lett. **50**, 2006 (1983).